Compensation of Intermodal Dispersion by Splicing Two Graded-Index Multimode Fibers

KATSUMI MORISHITA, MEMBER, IEEE, HIROSHI IKEDA, AND NOBUAKI KUMAGAI, FELLOW, IEEE

Abstract—**The deviations from the group delays expected for the optimum power-law index profile are numerically calculated for several types of undesired fibers using a scalar multilayer approximation method. This paper shows the way two fibers are selected from among undesired fibers so that the fiber spliced to each other becomes broad band.**

I. Introduction

MUCH EFFORT has been expended on designing multimode optical fibers that will have sufficient information-carrying capacity. However, manufactured fibers have various impulse responses and bandwidths because of departures of the index profile from its optimum shape. It is important to use fabricated fibers with narrow bandwidth from the practical point of view. We know that splicing graded-index fibers brings about the compensation of intermodal dispersion and reduces the pulse broadening in the spliced fibers [1]–[3].

It is the purpose of this paper to calculate the group delays for various nonoptimum index profiles and the mode conversion coefficients at the joint and indicate the way two fibers are selected from the nonoptimum fibers so that the fiber spliced to each other becomes broad band. The group delays and impulse responses are computed for the optimum power-law refractive-index fiber. Then the group delays are numerically analyzed for the various deformed profiles, i.e., nonoptimum power-law profiles, power-law profiles with a central dip and hump, and index perturbations near core-cladding interface [4], [5]. On the basis of the knowledge of the calculated group delays, we select two fibers from among the undesired fibers to reduce the pulse broadening in the spliced fiber. The impulse responses and the pulsewidths are then calculated for the deformed and the spliced fibers.

II. Scalar Multilayer Approximation Method

Since exact analysis for graded-index optical fibers is difficult and time-consuming, appropriate approximation techniques have been developed. Among them, scalar approximation analysis is one of the most widely used techniques. The accuracy of scalar approximation technique in optical fiber analysis was investigated in detail [6], [7]. In this paper, we use the scalar multilayer approximation method [8] to obtain easily the mode conversion coefficients at the joint between two graded-index fibers without offset, tilt, and spacing.

It is assumed that the permittivity of the fiber depends only upon the distance r from the axis, and the permeability is equal to that of vacuum μ_0. The refractive-index profile in the core region is represented approximately by a stratified multilayer structure. Applying the scalar approximation conditions into Maxwell's equations, we get the following scalar wave equation in the ith layer:

$$\frac{d^2\phi}{dr^2}+\frac{1}{r}\frac{d\phi}{dr}+\left(k^2n_i^2-\beta^2-\frac{m^2}{r^2}\right)\phi=0 \qquad (1)$$

where $k=\omega\sqrt{\varepsilon_0\mu_0}$, and β, n_i, and m are a propagation constant of the guided mode, the refractive-index of the ith layer, and an azimuthal quantum number, respectively. The solutions of (1) are represented exactly by Bessel functions, and ϕ and $d\phi/dr$ in the ith layer are expressed as

$$\begin{bmatrix}\phi\\ \frac{1}{\beta}\frac{d\phi}{dr}\end{bmatrix}=\begin{bmatrix}Z_m(u_ir) & \bar{Z}_m(u_ir)\\ \frac{u_i}{\beta}Z'_m(u_ir) & \frac{u_i}{\beta}\bar{Z}'_m(u_ir)\end{bmatrix}\begin{bmatrix}A_i\\ B_i\end{bmatrix} \qquad (2)$$

where A_i and B_i are unknown coefficients, and Z_m and $\bar{Z}_m$ are signified as follows:

i) $Z_m(u_ir)=J_m(u_ir)$ $\quad \bar{Z}_m(u_ir)=N_m(u_ir)$, for $u_i^2=k^2n_i^2-\beta^2>0$

ii) $Z_m(u_ir)=I_m(u_ir)$ $\quad \bar{Z}_m(u_ir)=K_m(u_ir)$, for $-u_i^2=k^2n_i^2-\beta^2<0$.

Using that ϕ and $d\phi/dr$ are continuous across the boundary of each layer, the propagation constants and the coefficients (A_i, B_i) can be obtained.

The group velocity V_g obtained by the scalar approximation method is expressed as [9]

$$\frac{V_g}{C}=\frac{\beta}{k}\frac{\int_0^\infty \phi^2 r\,dr}{\int_0^\infty n\frac{d(kn)}{dk}\phi^2 r\,dr} \qquad (3)$$

where C is the velocity of light in vacuum. At the junction of two graded-index fibers, I and II, the mode conversion

Manuscript received August 31, 1981; revised December 9, 1981.
K. Morishita is with the Department of Precision Engineering, Osaka Electro-Communication University, Neyagawa, Osaka 572, Japan.
H. Ikeda is with Asahi Broadcasting Company, Osaka, Japan.
N. Kumagai is with the Department of Electrical Communication Engineering, Osaka University, Osaka 565, Japan.

0018-9480/82/0500-0694$00.75 ©1982 IEEE

coefficient $C_{mnm'n'}$ from LP_{mn} mode in line I to $LP_{m'n'}$ mode in line II is represented approximately as

$$C_{mnm'n'}=\frac{\left(\int \Phi^{\mathrm{I}}_{mn}\Phi^{\mathrm{II}}_{m'n'}\,ds\right)^2}{\int \Phi^{\mathrm{I}^2}_{mn}\,ds\int \Phi^{\mathrm{II}^2}_{m'n'}\,ds} \tag{4}$$

where Φ^{I}_{mn} and $\Phi^{\mathrm{II}}_{m'n'}$ are the field distributions of LP_{mn} mode in line I and $LP_{m'n'}$ mode in line II, respectively. The refractive-index in multilayer approximation analysis is constant in each layer. Therefore, the expression for the group velocity, (3), and the mode conversion coefficient without offset, (4), can be rewritten in the forms

$$\frac{V_g}{C}=\frac{\beta}{k}\frac{\sum_l I_l}{\sum_l\left(n_l^2-n_l\lambda\frac{dn_l}{d\lambda}\right)I_l} \tag{5}$$

$$C_{mnmn'}=\frac{\left(\sum_l L_l\right)^2}{\left(\sum_l J_l\right)\left(\sum_i K_l\right)} \tag{6}$$

where

$$I_l=\int_{a_{l-1}}^{a_l}\{A_lZ_m(u_lr)+B_l\bar{Z}_m(u_lr)\}^2 r\,dr$$

$$J_l=\int_{a_{l-1}}^{a_l}\{A_l^{\mathrm{I}}Z_m(u_l^{\mathrm{I}}r)+B_l^{\mathrm{I}}\bar{Z}_m(u_l^{\mathrm{I}}r)\}^2 r\,dr$$

$$K_l=\int_{a_{l-1}}^{a_l}\{A_l^{\mathrm{II}}Z_m(u_l^{\mathrm{II}}r)+B_l^{\mathrm{II}}\bar{Z}_m(u_l^{\mathrm{II}}r)\}^2 r\,dr$$

$$L_l=\int_{a_{l-1}}^{a_l}\{A_l^{\mathrm{I}}Z_m(u_l^{\mathrm{I}}r)+B_l^{\mathrm{I}}\bar{Z}_m(u_l^{\mathrm{I}}r)\}\times\{A_l^{\mathrm{II}}Z_m(u_l^{\mathrm{II}}r)+B_l^{\mathrm{II}}\bar{Z}_m(u_l^{\mathrm{II}}r)\}r\,dr.$$

Since the integration I_l, J_l, K_l, and L_l can be analytically obtained, the group velocity V_g and the mode conversion coefficient $C_{mnmn'}$ are determined by using (5) and (6) without numerical integration.

It is assumed that all guided modes propagate independently from each other in lines I and II, and the attenuation constant and the group delay of LP_{mn} mode of each line are $\alpha^{\mathrm{I,II}}_{mn}$ and $\tau^{\mathrm{I,II}}_{mn}$. The output power transfered from LP_{mn} to $LP_{mn'}$, $P_{mnn'}$, the total output power P, the average delay time $\bar{\tau}$, and the rms pulsewidth σ, are given by

$$P_{mnn'}=C_{mnmn'}P_{0mn}e^{-(\alpha^{\mathrm{I}}_{mn}L_1+\alpha^{\mathrm{II}}_{mn'}L_2)} \tag{7}$$

$$P=\sum_{mnn'}P_{mnn'} \tag{8}$$

$$\bar{\tau}=\frac{\sum_{mnn'}\{(\tau^{\mathrm{I}}_{mn}L_1+\tau^{\mathrm{II}}_{mn'}L_2)P_{mnn'}\}}{P} \tag{9}$$

$$\sigma^2=\frac{\sum_{mnn'}\{\{(\tau^{\mathrm{I}}_{mn}L_1+\tau^{\mathrm{II}}_{mn'}L_2)-\bar{\tau}\}^2P_{mnn'}\}}{P} \tag{10}$$

where P_{0mn} is the incident power of LP_{mn}, and L_1 and L_2 are length of the fibers I and II, respectively.

III. Compensation of Intermodal Dispersion by Splicing

Index profiles of manufactured fibers deviate from the desired perfect index profile because of the difficulty of controlling its shape. Deviations of the index distribution from the optimum profile can take several forms, including undesired exponents of power-law profile, a central dip and hump, and an index rise and fall near core-cladding boundary (tail (+), (−)) given by (11)

$$n(r)=\begin{cases}n_0\left(\left\{1-2\Delta\left(\frac{r}{a}\right)^{\alpha}\right\}^{1/2}+\delta(r)\right), & \text{for core region}\\ n_0(1-2\Delta)^{1/2}=n_{\text{clad}}=1.453, & \text{for cladding region}\end{cases} \tag{11}$$

where $\Delta=0.01$, $a=25$ μm, and $\delta(r)$ is expressed as

$\delta(r)=0,$ for undesired exponents

$$\delta(r)=\begin{cases}\pm 0.1\Delta\left\{1-25\left(\frac{r}{a}\right)^2\right\}^{1/2}, & r\leqslant 0.2a\\ 0, & r>0.2a\end{cases}$$

for hump and dip (12)

$$\delta(r)=\begin{cases}\pm\left\{\left(\frac{30}{25}\right)^{\alpha}-1\right\}\Delta\left(\frac{25}{30}\frac{r}{a}\right)^6 \exp\left\{-500\left(1-\left(\frac{25}{30}\frac{r}{a}\right)\right)^5\right\}, & r\leqslant 1.2a\\ 0, & r>1.2a\end{cases}$$

for tail (+) and tail (−) (13)

and if $n(r)<n_{\text{clad}}$, $n(r)=n_{\text{clad}}$. The index profiles are shown in Fig. 1. It is the main purpose of this paper to calculate the group delays for several undesired fibers and describe how to select two fibers from the nonoptimum fibers so that the fiber spliced then becomes broad band.

In this numerical analysis, it is assumed that all guided modes propagate independently from each other except at spliced point and suffer the attenuation shown in Fig. 2 [10], and have input power shown in Fig. 3 [8], and fibers are made of GeO_2-doped fused silica. The group delay, the rms pulsewidth, the total loss, and the mode conversion coefficient are computed for the refractive-index profile divided into 50 layers in consideration of material dispersion of GeO_2-doped fused silica at $\lambda=0.83$ μm. The analyzed fibers have about 400 propagation modes.

A. Fibers with Power-Law Profile

The mode group delays for the fiber with optimum power-law profile ($\alpha=2.04$) are plotted versus the normalized principal mode number in Fig. 4. Modes near cutoff

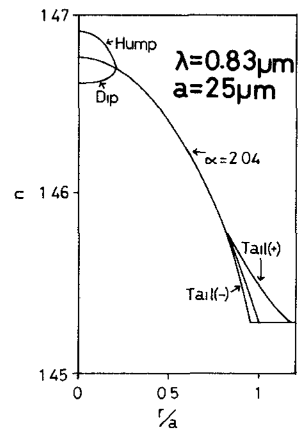

Fig. 1. Deviations of the index distribution from the optimum power-law profile ($\alpha = 2.04$).

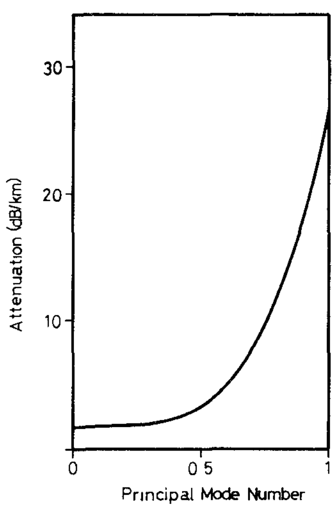

Fig. 2. Differential mode attenuation as a function of the normalized principal mode number.

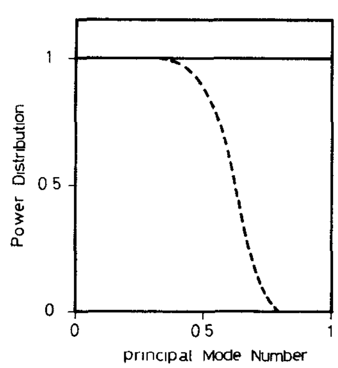

Fig. 3. Input modal power distribution. —— uniform excitation; ------ low-mode excitation. This means on-axis excitation with laser diode [8].

show large differences in group delay. However, modes near cutoff have little effect on the rms pulsewidth, because they usually have much loss and little excited power. Assuming that Figs. 2 and 3 show the attenuation and excited power of each guided mode, output pulses at propagation distance 1 km are computed as shown in Fig. 5. For uniform excitation, the rms pulsewidth σ looks bad for its pulse form. This is owing to near cutoff modes which are not written in Fig. 5 because of their little

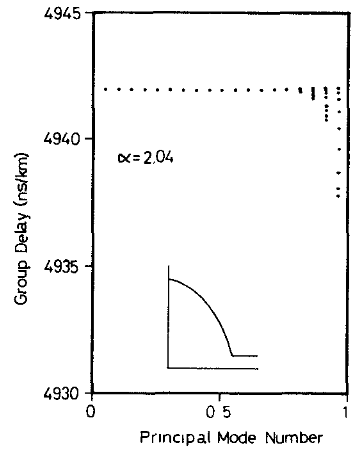

Fig. 4. Group delay as a function of the normalized principal mode number for the optimum power-law index fiber.

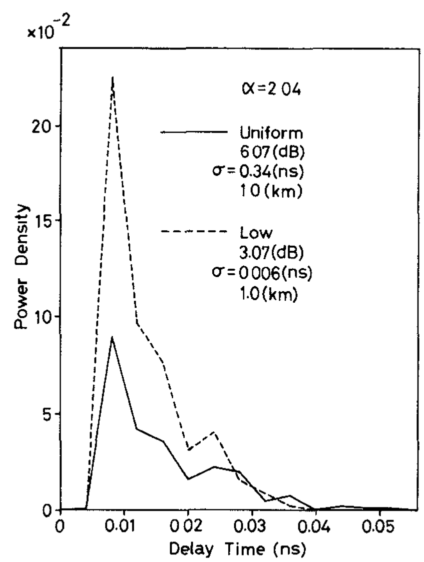

Fig. 5. Impulse responses of the fiber with the optimum power-law profile. —— uniform excitation; ------ low-mode excitation.

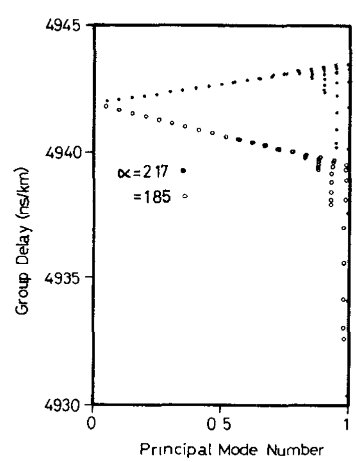

Fig. 6. Group delay as a function of the normalized principal mode number for power-law index fibers.

accepted power and large differences in group delay.

For fibers with smaller and larger power-law exponents than optimum one, the group delay decreases and increases about linearly with the principal mode number except for

TABLE I
MODE CONVERSION COEFFICIENT $C_{mnmn'}$ CAUSED BY SPLICING POWER-LAW INDEX FIBERS WITH $\alpha = 1.85$ AND 2.17

m	n \ n'	1	2	3	4	5	6	7	8	9	10
0	1	0.99	0.01	0	0	0	0	0	0	0	0
0	5	0	0	0	0.01	0.97	0.01	0	0	0	0
5	1	0.99	0.01	0	0	0	0	0	0	-	-
5	5	0	0	0	0	0.99	0	0	0	-	-
10	1	1.00	0	0	0	0	-	-	-	-	-
10	5	0	0	0	0	0.99	-	-	-	-	-

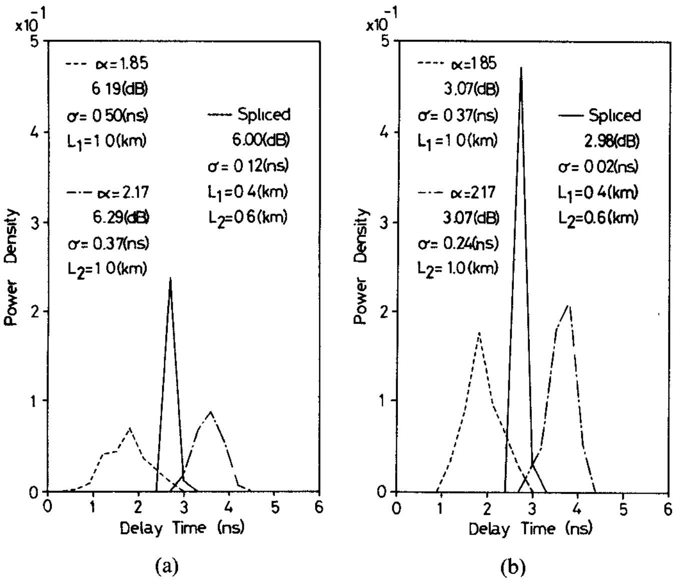

Fig. 7. Impulse responses of fibers with power-law profile and the spliced fiber. (a) Output pulses for uniform excitation. (b) Output pulses for low-mode excitation.

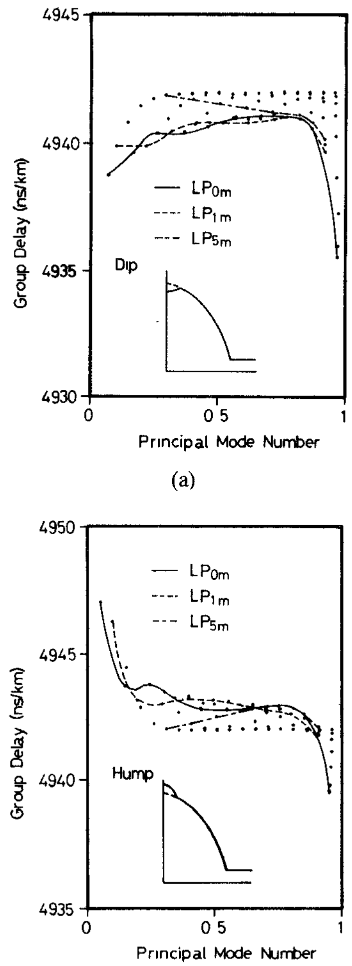

Fig. 8. Group delay as a function of the normalized principal mode number for the fibers with a central dip and hump on the optimum power-law profile. (a) Fiber with dip. (b) Fiber with hump.

near cutoff modes, respectively. As an example, fibers with power-law exponents $\alpha = 1.85$ and 2.17 are analyzed in this section. Fig. 6 shows the mode group delays versus the normalized principal mode number for fibers with power-law exponents $\alpha = 1.85$ and 2.17. The mode conversion coefficient $C_{mnmn'}$, which indicates the power ratio transfered from LP_{mn} in the fiber with $\alpha = 1.85$ to $LP_{mn'}$ in the fiber with $\alpha = 2.17$, is shown in Table I. The modes LP_{05}, LP_{55}, and LP_{105} have a 1-percent splice loss. It becomes evident that modes with high radial quantum number suffer a little splice loss and the mode conversion coefficient between modes with the same mode number is about unity. Therefore, we can get the fiber with much wider bandwidth by splicing to each other in a proper length ratio, which is determined by the ratio of the slope of the group delay versus principal mode number line. Output pulses at propagation distance 1 km are calculated for the fibers with $\alpha = 1.85$ and 2.17 and the spliced fiber in Fig. 7. Fig. 7(a) and (b) show the output pulses for uniform and low-mode excitations, respectively. The splicing reduces the pulsewidth to about one-third and one-tenth for the fiber with $\alpha = 2.17$, and about one-fourth and one-twentieth for the fiber with $\alpha = 1.85$ for uniform and low-mode excitations, respectively.

B. Fibers with Dip and Hump

The distorted power-law index fibers with a central dip and hump, which are shown in Fig. 1, are analyzed. The group delay of each propagation mode is computed for fibers with dip and hump on the optimum power-law index profile, and is shown in Fig. 8. Modes with low azimuthal quantum number are strongly perturbed by the central dip and hump. On comparison of Fig. 8(a) and (b), the group delays for the fibers with dip and hump turn out to show the negative and the positive deviations from the group delays expected for the optimum power-law profile, respectively. By means of splicing them, we can get the broadband fiber as a result of the compensation of intermodal dispersion.

Output pulses are computed for the fibers with dip and hump and the fiber spliced to each other, and are shown in Fig. 9. Fig. 9(a) and (b) indicate the output pulses for uniform and low-mode excitations, respectively. For both excitations, the splicing reduces the pulsewidth to about one-third and one-fourth for the individual fibers. The effect on the compensation of intermodal dispersion for the fibers with dip and hump is less than that for the pure power-law index fibers. It is due to large disparities in the

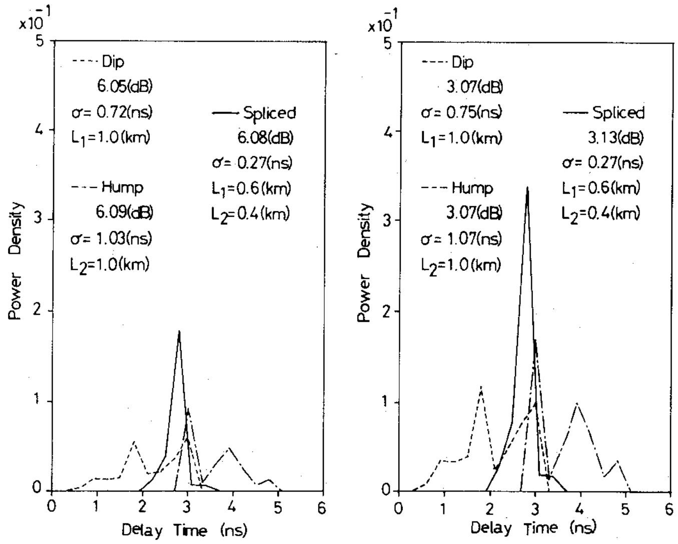

Fig. 9. Impulse responses of the fibers with a central dip and hump on the optimum power-law profile and the spliced fiber. (a) Output pulses for uniform excitation. (b) Output pulses for low-mode excitation.

TABLE II
MODE CONVERSION COEFFICIENT $C_{mnmn'}$ CAUSED BY SPLICING FIBERS WITH DIP AND HUMP

m	n \ n'	1	2	3	4	5	6	7	8	9	10
0	1	0.24	0.33	0	0	0	0	0	0	0	0
0	5	0	0.01	0.02	0.06	0.80	0.09	0.01	0	0	0
1	1	0.76	0.22	0.01	0	0	0	0	0	0	0
1	5	0	0.01	0.01	0.05	0.84	0.08	0.01	0	0	0
5	1	1.00	0	0	0	0	0	0	-	-	-
5	5	0	0	0	0	0.98	0.01	0	-	-	-

group delays and the mode conversion from modes with low azimuthal quantum number to modes with other mode number, which is shown in Table II. The mode LP_{01} has a 43-percent splice loss. The modes with low azimuthal and low radial quantum number suffer much splice loss because they have a large portion of the whole power in the vicinity of fiber axis.

C. *Fibers with Tail*

The change of the group delay caused by tails, which are an index rise and fall near core-cladding boundary (tail (+), tail (−)) in Fig. 1, is analyzed. Modes near cutoff are greatly affected by tails, as shown in Fig. 10. The group delays of modes near cutoff are decreased and increased by tail (+) and tail (−), respectively. Therefore, the pulse-width can be reduced by splicing the fibers with tail (+) and tail (−) by reason of the compensation of intermodal dispersion.

Output pulses are calculated for the fibers with tail (+) and tail (−) and the fibers spliced to each other, and are shown in Fig. 11. Fig. 11(a) and (b) indicate the output pulses for uniform and low-mode excitations. The length

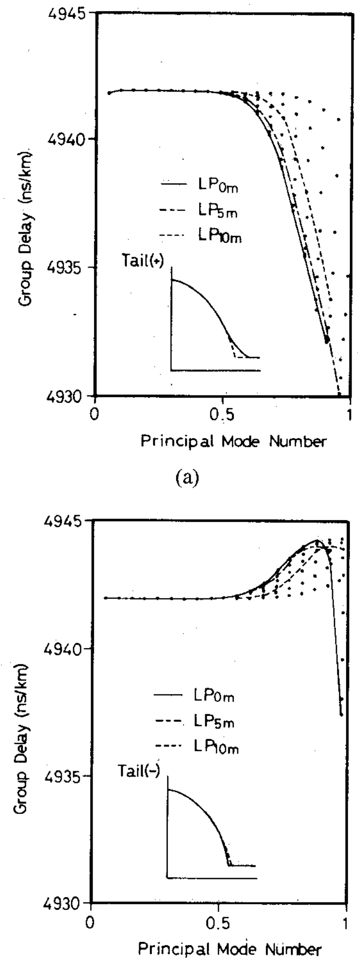

Fig. 10. Group delay as a function of the normalized principal mode number for the fibers with tails on the optimum power-law profile. (a) Fiber with an index rise near core-cladding boundary. (b) Fiber with an index fall near core-cladding boundary.

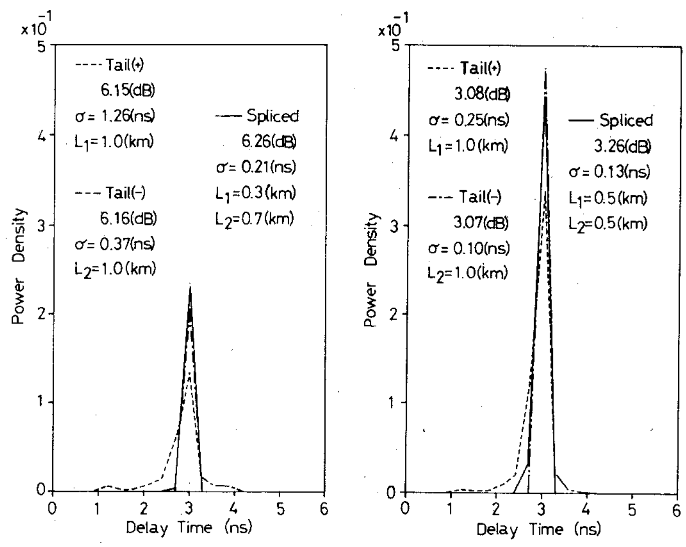

Fig. 11. Impulse responses of the fibers with tails on the optimum power-law profile and the spliced fiber. (a) Output pulses for uniform excitation. (b) Output pulses for low-mode excitation.

TABLE III
MODE CONVERSION COEFFICIENT $C_{mnmn'}$ CAUSED BY SPLICING FIBERS WITH TAILS

m	n \ n'	1	2	3	4	5	6	7	8
5	1	1.00	0	0	0	0	0	0	0
5	5	0	0	0	0	0.99	0.01	0	0
10	1	1.00	0	0	0	0	0	-	-
10	5	0	0	0	0.04	0.73	-	-	-
12	1	1.00	0	0	0	-	-	-	-
12	4	0	0	0.02	0.80	-	-	-	-

ratio of the individual fibers is changed for each excitation for the purpose of getting the large effect of the compensation of intermodal dispersion. For the fiber with tail (+), the splicing reduces the pulsewidth to about one-second and one-sixth for both excitations. The splicing, however, does not reduce the pulsewidth for the fiber with tail (−). The little reduction in pulsewidth results from the large difference in the group delay between modes with the same mode number in the fibers with tail (+) and tail (−). The most part of the incident power is converted into the guided mode with the same mode number at the junction, but modes with high azimuthal and high radial quantum numbers suffer about 20-percent splice loss, as shown in Table III. The fiber with tail (−), therefore, can be more improved by splicing with the fiber with a small index rise near core-cladding boundary. In the case of the deformation near core-cladding boundary, however, reduction in pulsewidth by means of splicing seems not to be expected much for a usual excitation due to much loss and little excitation power of modes near cutoff.

D. Fibers with Various Index Deformations

Fabricated fibers take different forms of index deformations, including undesired exponents of power-law profile, a central dip and hump, and an index rise and fall near core-cladding boundary, as shown in *A*, *B*, and *C*. In the case that the index deformations happen at the same time, deviations from the group delays expected for the optimum profile are about additions of that caused by each deformation [5]. We, therefore, consider that the fibers with the hump and undesired exponent $\alpha = 1.85$ and with the dip and $\alpha = 2.17$ are presumably the best or better pairs for reduction in pulsewidth.

The variation from the optimum group delays increases with the magnitudes and radii of dip, hump, and tail. The group delay variations, however, are similar in shape for the same kind of index deformations. The nonoptimum fibers can be classified into some groups according to index deformations, i.e., dip, hump, tail, larger, and smaller exponents than optimum one, and combinations of them. Splicing fibers belonging to the same group does not reduce the pulsewidth, and is equivalent to strengthening the magnitude of index deformations. The mode dispersion characteristics of fabricated fibers can be improved by splicing fibers of the groups with opposite trends in refractive index profile, including splicing fibers of the same group if necessary.

IV. CONCLUSIONS

Manufactured fibers have various departures of the index profile from its optimum shape because of the difficulty of controlling its shape. The deviations from the group delays expected for the optimum power-law index profile have been calculated for several types of undesired fibers. We have described the way two fibers are selected from the nonoptimum fibers so that splicing to each other reduces the pulsewidth. The various deformed profiles analyzed in this paper are nonoptimum power-law profiles, power-law profiles with a central dip and hump, and an index rise and fall near core-cladding boundary. As a result of this computation, it can be concluded that splicing the fibers with the opposite departures from the optimum index profile reduces the pulsewidth because of the compensation of intermodal dispersion.

REFERENCES

[1] M. Eve, "Multipath time dispersion theory of an optical network," *Opt. Quantum Electron.*, vol. 10, p. 41, Jan. 1978.
[2] T. Matsumoto and K. Nakagawa, "Wavelength dependence of spliced graded-index multimode fibers," *Appl. Opt.*, vol. 18, no. 9, p. 1449, May 1979.
[3] Y. Daido, "Refractive index profiling of graded-index fibers to attain a 100-MHz bandwidth at a fiber length of 100 km," *Trans. Inst. Electron. Commun. Eng. Japan*, vol. E64, no. 1, p. 13, Jan. 1981.
[4] K. F. Barrell and C. Pask, "Pulse dispersion in optical fibers of arbitrary refractive-index profile," *Appl. Opt.*, vol. 19, no. 8, p. 1298, Apr. 1980.
[5] M. D. Feit and J. A. Fleck, "Mode properties and dispersion for two optical fiber-index profiles by the propagating beam method," *Appl. Opt.*, vol. 19, no. 18, p. 3140, Sept. 1980.
[6] K. Morishita, Y. Kondoh, and N. Kumagai, "On the accuracy of scalar approximation technique in optical fiber analysis," *IEEE Trans. Microwave Theory Tech.*, vol. MTT-28, p. 33, Jan. 1980.
[7] K. Morishita, Y. Obata, and N. Kumagai, "Accuracy of the group velocity of the step-index fiber modes evaluated by the scalar approximation technique," *Trans. Inst. Electron. Commun. Eng. Japan*, vol. 64-B, no. 1, p. 87, Jan. 1981 (in Japanese).
[8] K. Morishita, "Numerical analysis of pulse broadening in graded-index optical fibers," *IEEE Trans. Microwave Theory Tech.*, vol. MTT-29, p. 348, Apr. 1981.
[9] K. M. Case, "On wave propagation in inhomogenious media," *J. Math. Phys.*, vol. 13, no. 3, p. 360, Mar. 1972.
[10] K. Kitayama, M. Tateda, S. Seikai, and N. Uchida, "Determination of mode power distribution in a parabolic-index optical fibers: Theory and application," *IEEE J. Quantum Electron.*, vol. QE-15, p. 1161, Oct. 1979.

Katsumi Morishita (S'74–M'77) was born in Fukui, Japan, on February 24, 1949. He received the B.E., M.E., and Ph.D. degrees in electrical communication engineering from Osaka University, Osaka, Japan, in 1972, 1974, and 1977, respectively.

From 1977 to 1978 he was a Postdoctoral Fellow of the Japan Society for the Promotion of Science. Since 1981 he has been with Osaka Electro-Communication University, Neyagawa, Osaka, Japan, where he is now a Lecturer of the Department of Precision Engineering. His research interests are in the areas of electromagnetic field analyses and optical waveguides.

Dr. Morishita is a member of the Institute of Electronics and Communication Engineers of Japan and the Society of Instrument and Control Engineers of Japan.

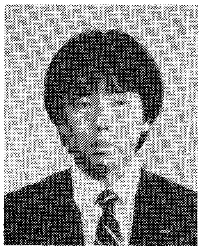

Hiroshi Ikeda was born in Kobe, Japan, on October 28, 1957. He received the B.E. degree in electrical communication engineering from Osaka University, Osaka, Japan, in 1981. He worked there on research in the areas of electromagnetic theory and optical waveguides.

He is presently with Asahi Broadcasting Company, Osaka, Japan.

Nobuaki Kumagai (M'59–SM'71–F'81) was born in Ryojun, Japan, on May 19, 1929. He received the B. Eng. and D. Eng. degrees from Osaka University, Osaka, Japan, in 1953 and 1959, respectively.

From 1956 to 1960 he was an Assistant Professor of Communication Engineering Department at Osaka University, Osaka, Japan. From 1958 through 1960 he was a Visiting Senior Research Fellow at the Electronics Research Laboratory of the University of California, Berkeley, on leave of absence from Osaka University. From 1960 to 1970 he was an Associate Professor, and has been a Professor of Communication Engineering at Osaka University since 1971. He served as a Department Chairman in the periods of 1972-1973 and 1977-1978. Since 1980 he was installed as the Dean of Student Affairs of Osaka University, serving concurrently as Professor of Communication Engineering.

His fields of interest are theory of electromagnetic fields and waves, microwaves, millimeter-waves, acoustic-waves engineering, optical fibers, optical integrated circuits and devices, lasers and their applications. He published more than one hundred technical papers in established journals on these topics. He is the co-author of *Microwave Circuits* (OHM-sha, Tokyo, 1963) and *Introduction to Relativistic Electromagnetic Field Theory* (Corona Publishing Co., Tokyo, 1971). From 1979 to 1981 he was President of the Microwave Theory and Techniques Society of the Institute of Electronics and Communication Engineers of Japan.

Dr. Kumagai is a member of the Institute of Electronics and Communication Engineers of Japan, the Institute of Electrical Engineers of Japan, and the Laser Society of Japan.

Slow Wave Gyrotron Amplifier with a Dielectric Center Rod

JOON Y. CHOE, HAN S. UHM, AND SAEYOUNG AHN, MEMBER, IEEE

Abstract—**The broad-band capability of the gyrotron amplifier with a dielectric center rod is investigated. The dispersion relation for the TE mode perturbation is obtained, and the system parameters for the optimum bandwidth are obtained for a small axial velocity spread. It is found that the dielectric center rod extends the frequency range of the intermediate wavelength mode (IWM), and reduces the contribution of the troublesome short wavelength mode (SWM). The bandwidth and the gain due to the IWM for the center rod geometry are superior to those for the wall clad dielectric gyrotron.**

I. INTRODUCTION

RECENTLY there have been numerous studies [1]–[6] on the dielectric loaded gyrotron for a wide-band application. It has been found [2], [4], [6] that there exist three unstable modes characterized by their axial phase velocities (v_{ph}); the long wavelength mode (LWM, $v_{ph} > c$), the intermediate wavelength mode (IWM, $c > v_{pn} > c\epsilon^{-1/2}$), and the short wavelength mode (SWM, $v_{ph} < c$). Here ϵ and c are the dielectric constant and the velocity of light. For a small axial velocity spread ($\lesssim 1$ percent), two slow wave modes (IWM and SWM) yield very promising bandwidth capability [2], especially when two modes are mixed by placing the beam close to the axis [4], [6]. However, the nature of the SWM [2], [4], whose perturbed fields are almost entirely supported by the electron beam, not by the waveguide, raises the difficulties related to the excitation and collection of the electromagnetic waves [2], [4]. One possible solution to this difficulty is to utilize the dielectric material as a center rod [7], rather than as an outside wall loading [1]–[5]. By using dielectric material as a center rod, it will be shown that the frequency range of the IWM is extended, while the contribution of the troublesome SWM is minimized.

Manuscript received August 18, 1981; revised October 28, 1981. This research was supported in part by an Independent Research Fund at the Naval Surface Weapons Center, and in part by the Office of Naval Research.

J. Y. Choe and H. S. Uhm are with the Naval Surface Weapons Center, White Oak, Silver Spring, MD 20910.

S. Ahn is with the Naval Research Laboratory, Washington, D.C. 20375.